2

X-671-72-437

PREPRINT

NASA TM X- 66266

THE LAST BALMER LINE AND Hγ IN MODEL B STARS

(NASA-TM-X-66266) THE LAST BALMER LINE AND H GAMMA IN MODEL B STARS (NASA) 24 p HC $3.25 CSCL 03B

N73-26840

Unclas
G3/30 07462

DAVID FISCHEL
DANIEL A. KLINGLESMITH

NOVEMBER 1972

GSFC

GODDARD SPACE FLIGHT CENTER
GREENBELT, MARYLAND

THE LAST BALMER LINE AND Hγ IN MODEL B STARS

by

David Fischel
and
Daniel A. Klinglesmith

Laboratory for Optical Astronomy
Goddard Space Flight Center

Received: 1972 October 13

Running Title: Last Balmer Line

ABSTRACT

Profiles of the last few Balmer lines (H_{12}-H_{27}) and the full profiles of the Hγ line were computed for a grid of hydrogen line blanketed model atmospheres. The use of the last hydrogen line and the equivalent width of Hγ provide a quick means of estimating the effective temperature and surface gravity of B stars. Regression curves relating the quantum number of the last hydrogen line to the electron density in the model atmosphere are given.

Furthermore, it is shown that the difference in the gravity determination deduced from Hγ equivalent widths using the Edmonds-Schlüter-Wells formalism and the Griem wing formulae is, at worst, 0.18 in the common logarithm.

Subject Headings: Atmospheres, Stellar--Early-Type Stars--Line Profiles

I. INTRODUCTION

In the course of a study of Bp stars (Klinglesmith, 1972), it was noted that the high hydrogen lines looked markedly different from those of normal main-sequence B stars. It was hoped that the last hydrogen line and the application of the Inglis-Teller (1939) formula would be an indicator of chemical composition peculiarities. Preliminary calculations indicated that this was so; although the final results, as described below, revealed a more complex behavior.

II. THEORY

The model atmospheres were taken from Klinglesmith (1971). They are hydrogen line (Lyman and Balmer) blanketed models in hydrostatic, radiative and local thermodynamic equilibrium covering the effective temperature range 10,000 (2,000) 20,000°K and the log g range 2.5 (0.5) 4.5 for hydrogen mass fractions of 0.0164, 0.143, 0.667 and 1.0.

The absorption coefficient for the high Balmer lines is the sum over the contributions of individual lines for which we use the formulae and table of $T(\beta, \gamma)$ from Griem (1960) with the corrections as noted by Griem (1962, 1967). The $H\gamma$ profiles were calculated using the Edmonds, Schlüter and Wells (1967) formalism. In addition, profiles using the Griem wing formula were calculated for the models with $X = 2/3$. We found it convenient to rewrite the wing formula as (in the notation of Griem, 1967)

$$I(\Delta\lambda) = N_e I_{qs}(\Delta\lambda)[N_i/N_e + E + (1-E)R(N, T)] \tag{1}$$

where N_e and N_i are the electron and ion densities, E is the ratio of the number of quasi-static perturbers to the number of electrons (eq. [8] of Griem, 1967)

$$E = 1 + 2\pi^{-1/2}\int_0^{y_1} y^{1/2}e^{-y}dy, \quad y_1 = b^2hc\ \Delta\lambda \quad /2\lambda^2kT \tag{2}$$

The quasi-static line shape factor is given by

$$I_{qs}(\Delta\lambda) = (3\pi/4)(2a_o^2R_\infty)^{3/2}(\lambda^3/\Delta\lambda^{5/2})(b^2-a^2)^{3/2} \tag{3}$$

and the quantity

$$R(N,T) = (32/\pi^3)^{1/2} \frac{b^3f(a,b)}{(b^2-a^2)^{3/2}} \left(\frac{\Delta\lambda}{\Delta\lambda_w}\right)^{1/2} \cdot[1 + \ln(\Delta\lambda w/\Delta\lambda_a)] \tag{4}$$

where a, b are the lower and upper principal quantum numbers, f(a, b) is given by Table 1 of Griem (1967), a_o is the Bohr radius, R is the Rydberg constant, $\Delta\lambda_w = \lambda^2kT/chb^2$, $\Delta\lambda_p = \lambda^2(e^2N_e/\pi mc^2)^{1/2}$ and

$$\Delta\lambda_a = \begin{cases} \Delta\lambda \text{ if } \Delta\lambda < \Delta\lambda p \\ \Delta\lambda_p \text{ if } \Delta\lambda \epsilon [\Delta\lambda_p, \Delta\lambda w] \\ \Delta\lambda_w \text{ if } \Delta\lambda > \Delta\lambda w \end{cases} \tag{5}$$

All the other symbols have their usual meaning. The value of $(32/\pi^3)^{1/2}$ is 1.032 and the quantity $b^3f(a, b)/(b^2-a^2)^{3/2}$ is 1.0235 for Hγ, decreasing to 1 as b increases.

These equations are algebraically identical to Griem

(1960, 1962, 1967), but computationally more convenient. Figure 1 illustrates $\log_{10}\chi$ calculated with these equations for $T = 10^4$ °K as a function of wavelength and electron pressure. The Inglis-Teller effect, which relates the upper quantum number of the last observable hydrogen line to electron density is clearly seen in this figure. The opacity in line center of H_{24} is appreciable compared to its wings at $\log P_e = 0.0$ and negligible at $\log P_e = 1.0$ whereas at H_{19} the line opacity does not disappear until $\log P_e = 1.5$.

III. RESULTS

Analysis of high dispersion spectrograms showed that the last visible Balmer line was roughly characterized by its line center being depressed ~5% from the sloping "continuum" over the blended Balmer lines. In order to avoid correlating a discrete integer variable with a continuous variable (the electron density), we defined the quantum number of the last visible Balmer line as the line whose upper quantum number, which, interpolated, would have had exactly a 5% depression at line center, i.e. n(5%). We also studied n(20%), but found it an insensitive parameter.

Table 1 lists the results of the calculations. Column 1 is the effective temperature of the model in units of 10^3 °K, column 2 is the model log g and columns 3, 4 and 5 are the n(5%)'s for models with X = 0.143, 2/3 and 1, respectively. Similarly, columns 6, 7 and 8 are the equivalent widths of Hγ by the ESW formalism; whereas column 9 is the equivalent width of Hγ by the Griem theory for models with $X = 2/3$. Column 10 is the percentage difference between the ESW and Griem results (columns 7 and 9) in the sense (ESW - Griem)/ESW. Column 11 is the difference in log g from the model value if one were to fit the Griem result (column 9) to the "observed" ESW result (column 7). It is clear from columns 10 and 11 that the observational uncertainty is as significant as the broadening theory differences in determining log g. Figure 2 shows the temperature averages of $\Delta W(H\gamma)$ and Δ log g. Since equivalent widths are not the best measure for determining the gravity, we also show the comparison of ESW and Griem profiles in Figure 3 for the 16,000^{o}K, log g = 4.0 model. Both the Griem and ESW profiles are shown as well as their difference. Similar plots were made of all the models referred to in Table 1; figure 3 is the worst case. In more than 90% of the models the differences between the two profiles is less than 0.025 in the residual intensity.

Figure 4 illustrates $W(H\gamma)$ versus n(5%) for the $X = 2/3$ models. The lines of constant gravity and constant effective temperature are indicated. Similar plots can be made for the other values of X. The dashed lines in figure 4 are estimates of where the curves would go if the hydrogen line blanketed LTE models were valid in those regions of the T_{eff} - log g plane. Stars for which the last hydrogen line have been measured (Unsöld and Struve, 1939) have been placed in figure 4, where the W(Hγ) values are from Petrie (1953, 1965), Petrie and Maunsell (1950), Petrie and Moyls (1956), MacDonald (1953) and Williams (1936). A comparison between the T_{eff} and log g determined from this graph and the work of Schild, Peterson, and Oke (1971) and Heintze (1968) is given in Table 2. Column 1 is the star name, column 2 and 3 are the T_{eff} and log g determined from Figure 4, column 4 is Heintze's T_{eff} at log g = 4.0 and columns 5 and 6 are the T_{eff} and log g determined by Schild,et al. One type of chemical composition peculiarity, namely helium under-abundance, is characterized by the UBV colors implying an earlier spectral type than the MK spectral classification. Table 3 lists helium poor stars (Nesterczuk, 1971) which are also plotted on Figure 4. It is apparent from Table 2 and Figure 4 that strong composition anomalies can be detected from spectra alone. If, for example, 36 Lyn were really an A1 star, it would lie near α Lyr and α Cma in Figure 4 for normal composition stars, However, Hγ and the last Balmer line indicate that, for X = 2/3, 36 Lyn should be about a 15,000^{o}K, log g = 4.0 star; i.e., B5V or B6V which is obviously inconsistent. Figure 5 incorporates the visual determination of the last hydrogen line by Unsöld and Struve (1939) with n(5%) (X = 2/3) using the Morton and Adams (1968) temperature scale and MK spectral types from the Yale Bright Star Catalog. The solid lines are lines of constant log g. This figure shows very clearly the surface gravities associated with each luminosity class. Thus with one spectrogram of moderate dispersion (20Å/mm - 40Å/mm) covering the region 3600Å - 4400Å; the position of a star in figures 4 and 5 could be determined and, barring severe composition peculiarities, the star's effective temperature could be determined to within ~1000°K and its surface gravity to within ~0.3 in log g, which certainly is a good first estimate for a curve-of-growth analysis. In this age of fine analysis these estimates would provide a very reasonable starting point for a grid of models.

In order to perform a curve-of-growth analysis the electron density, N_e, is needed rather than the surface gravity. It was found that the upper quantum number of the last hydrogen line, n(5%) correlates very well with electron density. Figure 6 shows the electron density at a temperature equal to the effective temperature for each model versus n(5%). The two regression equations that fit the data are given in the figure. Other electron densities, $N_e(T_R)$, $N_e(\tau_0 = 0.4)$ and $N_e(\tau_0 = 0.1)$; where T_R is the reversing layer temperature ($0.8 \times T_{eff}$) and τ_0 is the optical depth at the standard wavelength (4000Å) were plotted in a similar manner, however, $N_e(T_{eff})$ produced the least variance and included the most models. It should be remembered that these regression equations are for the models. Several unpublished models (Klinglesmith, 1971) have been added. Six models, (20, 2.5), (20, 3.0), (20, 3.5), (18, 3.0), (18, 2.5) and (16, 2.5) are not in the regression because of their large variances.

As long as hydrogen is the dominant continuum opacity source the "last visible hydrogen line" will be formed in the same region as the continuum since the continuum opacity is composed of the Paschen continuum and the merging of the upper levels of hydrogen. However, when hydrogen no longer dominates, the last hydrogen line will, in general, be formed in a different region from the continuum, and therefore, we expect little correlation between n(5%) and $N_e(T_{eff})$ as is the case for the low gravity, high temperature models. Similarly, the 10,000^{o}K models differ from all the other models because H^- is still a significant enough absorber that the last hydrogen line is formed higher in the atmosphere. At $\tau_0(T_{eff})$, the (10, 4.5) model has ~10 times more H^- opacity than the (12, 4.5) model and ~30 times more than the (10, 2.5) model. The latter model lies almost on the regression line of the hotter models.

IV. CONCLUSIONS

We have shown that the last visible hydrogen line can be used to determine the electron density in the line forming region of a stellar atmosphere to within a factor of two. We have also shown that the last visible hydrogen line and the equivalent width of Hγ can be used to determine both the effective temperature and the surface gravities for B stars.

Earlier investigations of the last hydrogen line by van Dien (1949) and Mihalas (1966) are not really comparable to the present investigation. Miss van Dien used the early work of Pannekoek (1939) to determine gravities of stars observed by Yü (1926). Tracings of Yü's observations yield quantum numbers consistently lower than Struve and Unsold by two or more except for a few higher dispersion values which are approximately equal to Struve and Unsold's. Her theoretical calculations are lower yet. Mihalas' values for A stars are lower by 2 for main sequence stars and by 4 for giants than those of the present work. His calculations, however, are based upon models without Lyman line blanketing and therefore are not expected to be comparable.

It should be pointed out that this analysis was done with LTE, hydrogen line blanketed models. The effects of non-LTE and/or metal line blanketing have not been considered and remain to be done.

The authors gratefully wish to acknowledge an anonymous referee for encouragement, positive criticism and bringing our attention to an overlooked reference.

TABLE 1

Last Hydrogen Line and Hγ Equivalent Widths from Model Atmospheres

$T_e/10^3$	log g	n(5%) X=0.143	2/3	1	W_{ESW}(Hγ) X=0.143	2/3	1	W_G(Hγ)	ΔW	Δlog g
10	2.5	22.666	24.142	24.697	8.52	6.28	5.66	6.79	-0.081	0.110
	3.0	21.013	22.370	22.784	11.30	8.60	7.83	9.30	-0.081	0.125
	3.5	19.642	20.745	21.130	14.60	11.40	10.50	12.30	-0.079	0.128
	4.0	18.289	19.216	19.641	18.50	14.90	13.80	15.90	-0.067	0.125
	4.5	16.863	17.860	18.245	22.70	18.90	17.70	20.00	-0.058	0.137
12	2.5	21.629	23.163	23.830	6.39	4.66	4.15	5.05	-0.084	0.113
	3.0	20.106	21.526	22.024	8.39	6.39	5.83	6.94	-0.086	0.131
	3.5	18.689	19.947	20.412	10.80	8.49	7.80	9.19	-0.082	0.152
	4.0	17.366	18.506	18.877	13.60	10.80	10.00	11.60	-0.074	0.138
	4.5	16.144	17.123	17.595	17.10	13.70	12.80	14.70	-0.073	0.172
14	2.5	20.887	22.586	22.968	5.06	3.68	3.24	3.99	-0.084	0.102
	3.0	19.448	20.802	21.274	6.88	5.20	4.74	5.67	-0.090	0.131
	3.5	18.088	19.272	19.771	8.36	7.00	6.43	7.60	-0.086	0.146
	4.0	16.805	17.908	18.371	11.50	9.05	8.40	9.78	-0.081	0.148
	4.5	15.656	16.711	16.987	14.40	11.50	10.70	12.40	-0.078	0.183
16	2.5	20.502	21.823	22.421	3.74	2.90	2.57	3.14	-0.083	0.083
	3.0	18.810	20.195	20.627	5.41	4.34	3.95	4.73	-0.090	0.123
	3.5	17.584	18.737	19.162	7.34	5.93	5.50	6.46	-0.089	0.151
	4.0	16.311	17.175	17.827	9.68	7.68	7.23	8.32	-0.083	0.139
	4.5	15.167	16.236	16.580	12.40	9.99	9.30	10.70	-0.071	0.154
18	2.5	19.226	21.194	21.880	2.46	2.20	1.99	2.37	-0.077	0.061
	3.0	18.166	19.698	20.193	3.89	3.60	3.34	3.93	-0.092	0.109
	3.5	16.936	18.347	18.706	5.63	5.11	4.47	5.57	-0.090	0.139
	4.0	15.897	16.902	17.446	7.76	6.76	6.37	7.33	-0.084	0.139
	4.5	14.801	15.827	16.170	10.30	8.81	8.26	9.48	-0.076	0.163
20	2.5	18.458	20.799	21.540	1.77	1.70	1.45	1.82	-0.076	0.045
	3.0	16.849	19.122	19.712	2.68	3.02	2.81	3.29	-0.089	0.102
	3.5	16.218	17.838	18.284	4.15	4.35	4.17	4.75	-0.092	0.128
	4.0	15.199	16.648	16.916	5.89	5.91	5.64	6.41	-0.085	0.134
	4.5	14.368	15.482	15.823	8.10	7.77	7.40	8.37	-0.077	0.161

TABLE 2

Comparison of Effective Temperatures and Surface Gravities

Star	$T_e/10^3$	log g	$T_e/10^3$ Heintze	$T_e/10^3$ Oke, Schild,	log g Peterson
ν Ori	27.2^{o}K	4.5	29.1^{o}K		
τ Sco	28.4	4.41	25.8		
φ Ori	25.6	4.18			
β Cep	23.8	3.85		24.2^{o}K	4.0
ϵ Per	23.8	3.85	25.4	28.6	4.0
γ Peg	20.8	3.77	20.4	21.7	4.0
β CMa	26.0	3.3			
102 Her	24.0	3.05			
ϵ CMa	26.0	2.95		28.6	4.0
ρ Leo	26.7	2.83			
κ Cas	22.5	2.54			
9 Cep	19.3	2.4			
ζ Cas	18.0	3.85			
τ Her	16.2	3.9	14.7		
ι Her	17.8	3.6	16.8		
ϵ Cas	17.6	3.6		15.9	4.0
η Lyr	17.5	3.25			
ζ Dra	18.0	2.85	13.2		
χ^2 Ori	17.0	2.1			
χ Aur	16.0	2.2			
β Ori	14.2	2.3			
55 Cyg	15.0	2.2			
4 Lac	12.0	<2.0			
ϵ Del	14.2	3.6			
67 Oph	16.0	2.6			
α Dra	10.1	3.75			
α Cma	9.8	4.0		10.2	4.35
α Lyr	9.7	3.9		9.65	4.05

TABLE 3

LAST HYDROGEN LINE AND Hγ EQUIVALENT WIDTHS
OBSERVED IN HELIUM-WEAK STARS

Star	Spectral Type	UBV Spectral Type	W(Hγ)	n(5%)	$Te/10^3$	log g	He/H
HD21699	B8 III	B5 IV	7.4	18.0	15.8	3.98	0.008
20 Eri	AO Si	B6 V	8.4	17.7	14.7	4.25	0.003
22 Eri	B8	B5 V	7.4	18.6	14.8	3.95	0.008
20 Tau	B7 III	B8 III	7.0	20.2	13.0	3.45	0.08
12 CMa	B7 III	B4 V	7.4	17.2	17.7	4.43	0.016
36 Lyn	A1	B7 IV	7.8	19.3	13.4	3.82	0.01

REFERENCES

Edmonds, F. M., Jr., Schluter, H., and Wells, D.C. 1967, M.N.R.A.S., 71, 271.

Griem, H. R. 1960, Ap. J., 132, 883.

__________ 1962, Ap. J., 136, 442.

__________ 1967, Ap. J., 147, 1092.

Heintze, J. R. W. 1968, B. A. N., 20, 1.

Hoffleit, D. 1964, Yale Bright Star Catalogue (New Haven, Conn.: Yale University Observatory) .

Inglis, D. R., and Teller, E. 1939, Ap. J., 90, 439.

Klinglesmith, D. A. 1971, Hydrogen-Line Blanketed Model Atmospheres, NASA SP-3065 (Washington: U.S. Government Printing Office).

__________ 1972, Ap. J., 171, 79

MacDonald, J. K. 1953, Pub. Dom. Ap. Obs., 9, 269.

Mihalas, D. 1966, Ap. J. Supp., 13, 1.

Morton, D. C., and Adams, T. F. 1968, Ap. J., 151, 611.

Nesterczuk, G. 1971, Master's Thesis, Univ. of Md.

van Dien, E. 1949, Ap. J. 109, 452.

Petrie, R. M. 1953, Pub. Dom. Ap. Obs., 9, 351.

__________ 1965, Pub. Dom. Ap. Obs., 18, 317.

__________, and Maunsell, C. O. 1950, Pub. Dom. Ap. Obs., 8, 253

__________, and Moyls, B. N. 1956, Pub. Dom. Ap. Obs., 10, 287.

Schild, R., Peterson, D.M., and Oke, J. B. 1971, Ap. J., 166,95.

Underhill, A. B. 1972, private communication.

Unsöld, A., and Struve, O. 1940, Ap. J., 91, 365.

Pannekoek, A. 1938, M.N.R.A.S., 98, 701.

Williams, E. G. 1936, Ap. J., 83, 305.

Yu, C. S. 1926, Lick Obs. Bull., # 375.

FIGURE TITLES

1. $\text{Log}_{10}\kappa$ (High Balmer lines only) versus $\log_{10} P_e$ and λ (Å) for $T = 10^4$ °K.
2. Temperature averages of $\Delta W(H\gamma)$ and $-\Delta \log g$ from Table 1.
3. Profiles of $H\gamma$ from the 16,000°K, log g = 4.0 model showing ESW and Griem as upper and lower curves. The difference is shown at the bottom. Note that the ΔR scale is expanded.
4. n(5%) versus W($H\gamma$) with stellar observations. Different luminosity classes are marked by separate symbols. Solid dots are the helium-weak stars.
5. n(5%) versus spectral type with the Strüve and Unsöld data using MK spectral types and the Morton-Adams temperature scale. Different luminosity classes are marked by separate symbols.
6. Log N_e (T_{eff}) versus log n(5%) from the models.

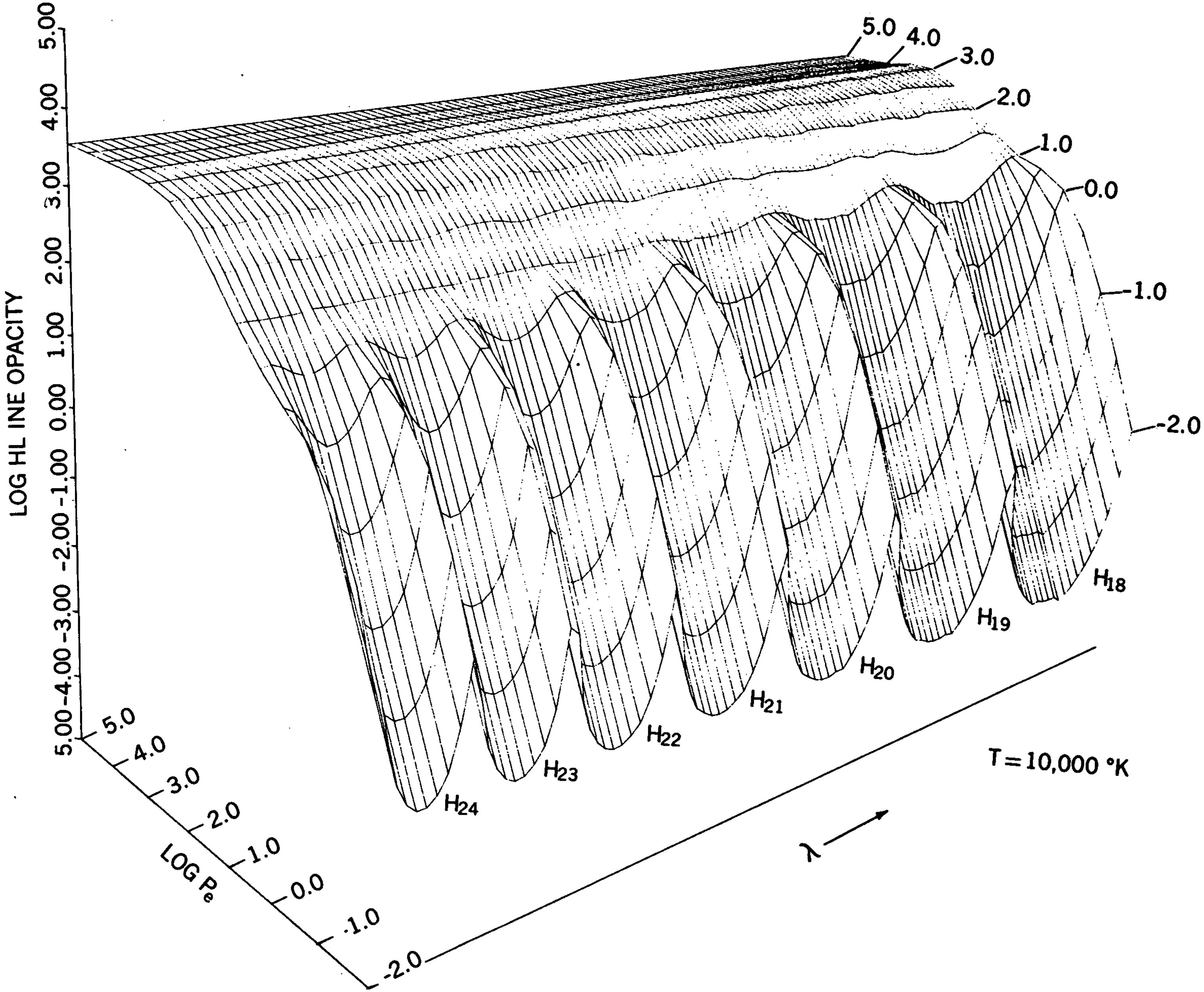
LOG HL INE OPACITY
5.00
4.00
3.00
2.00
1.00
0.00
-1.00
-2.00
-3.00
-4.00
-5.00
5.0
4.0
3.0
2.0
1.0
0.0
-1.0
-2.0
LOG P_e
5.0
4.0
3.0
2.0
1.0
0.0
-1.0
-2.0
H_{18}
H_{19}
H_{20}
H_{21}
H_{22}
H_{23}
H_{24}
T=10,000 °K
λ

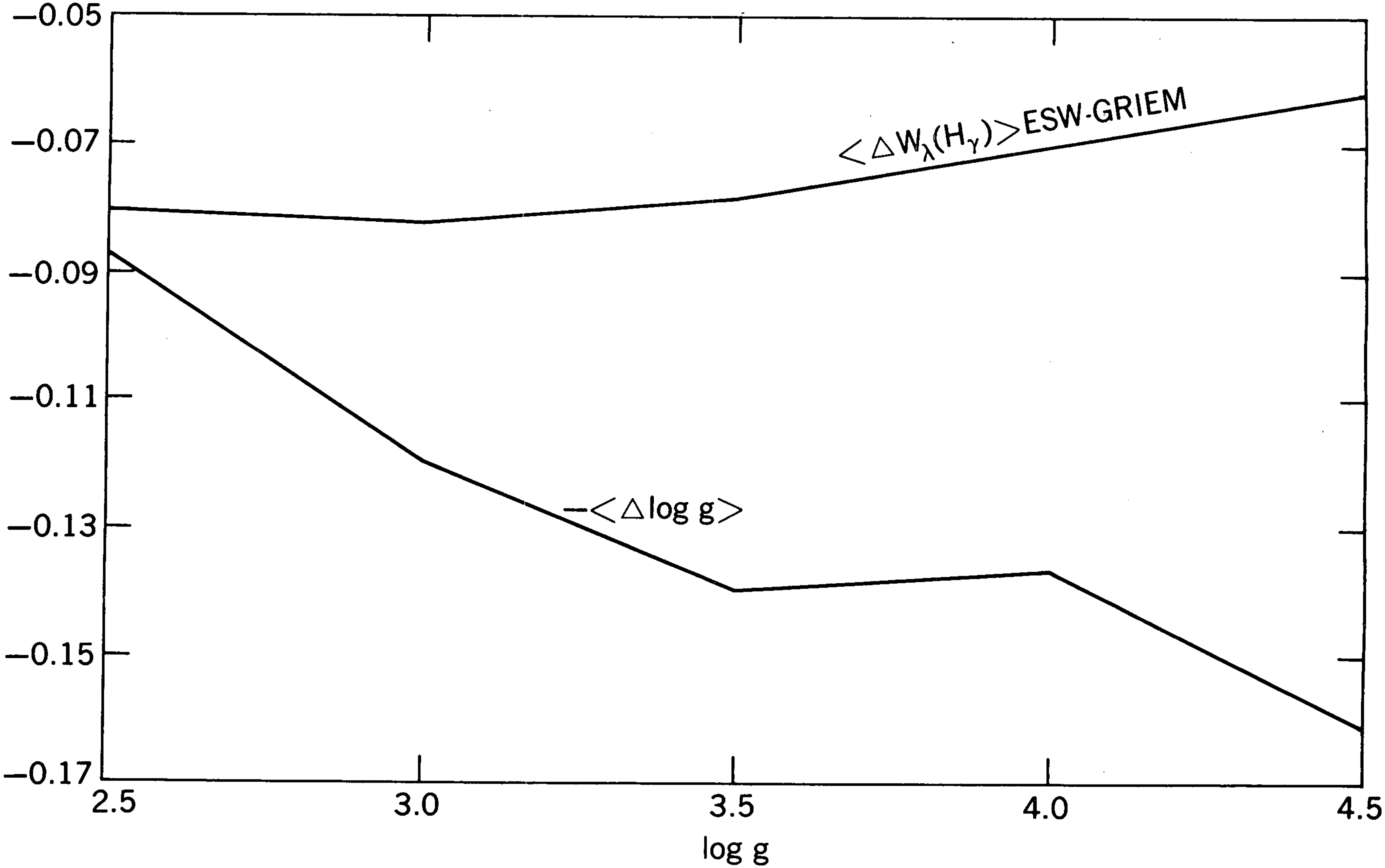
−0.05
−0.07
−0.09
−0.11
−0.13
−0.15
−0.17
2.5
3.0
3.5
4.0
4.5
log g
<ΔW$_\lambda$(H$_\gamma$)>ESW-GRIEM
−<Δlog g>

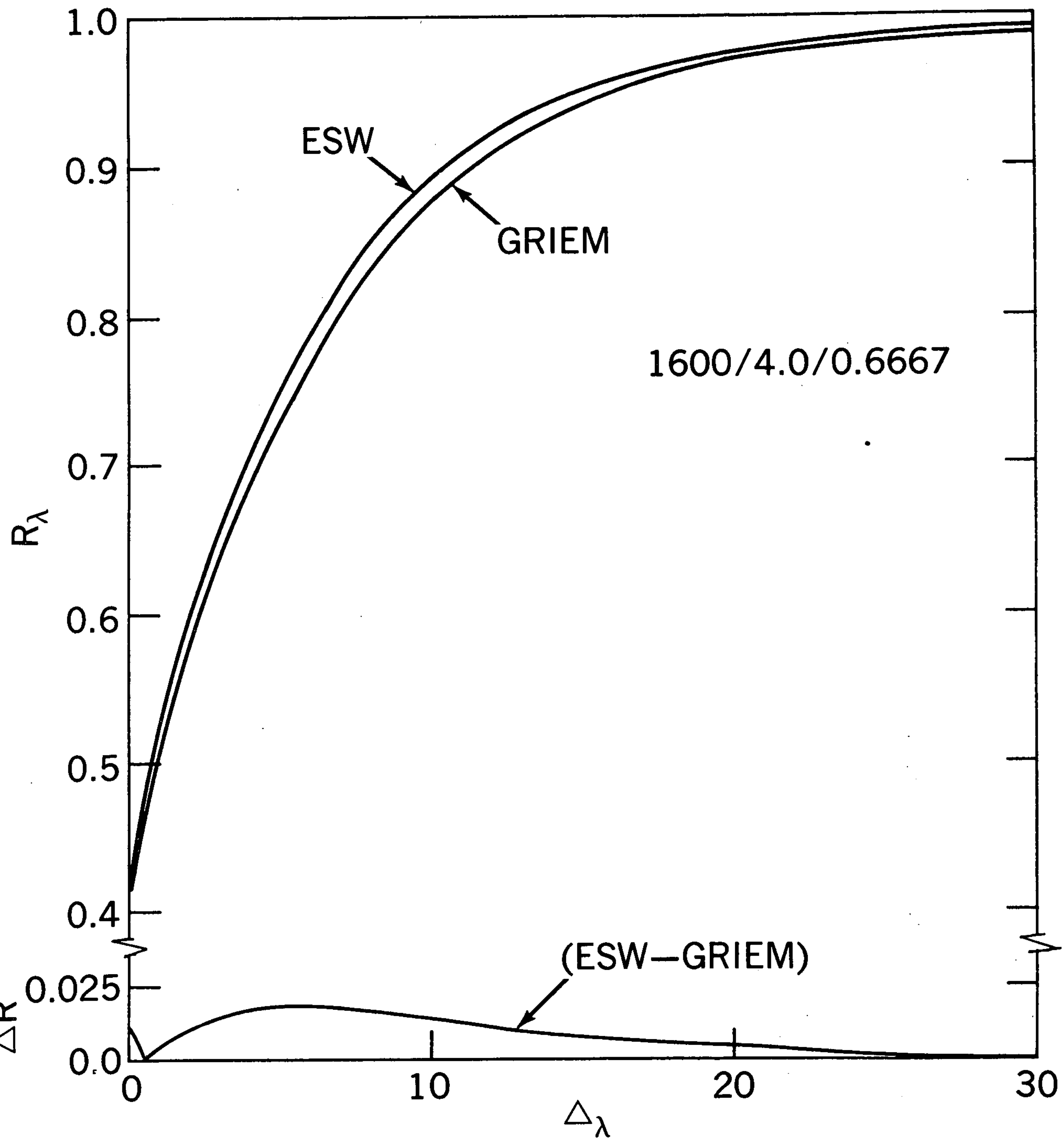
1.0
0.9
0.8
0.7
0.6
0.5
0.4
R_λ
ESW
GRIEM
1600/4.0/0.6667
(ESW—GRIEM)
ΔR
0.025
0.0
0
10
20
30
Δ_λ

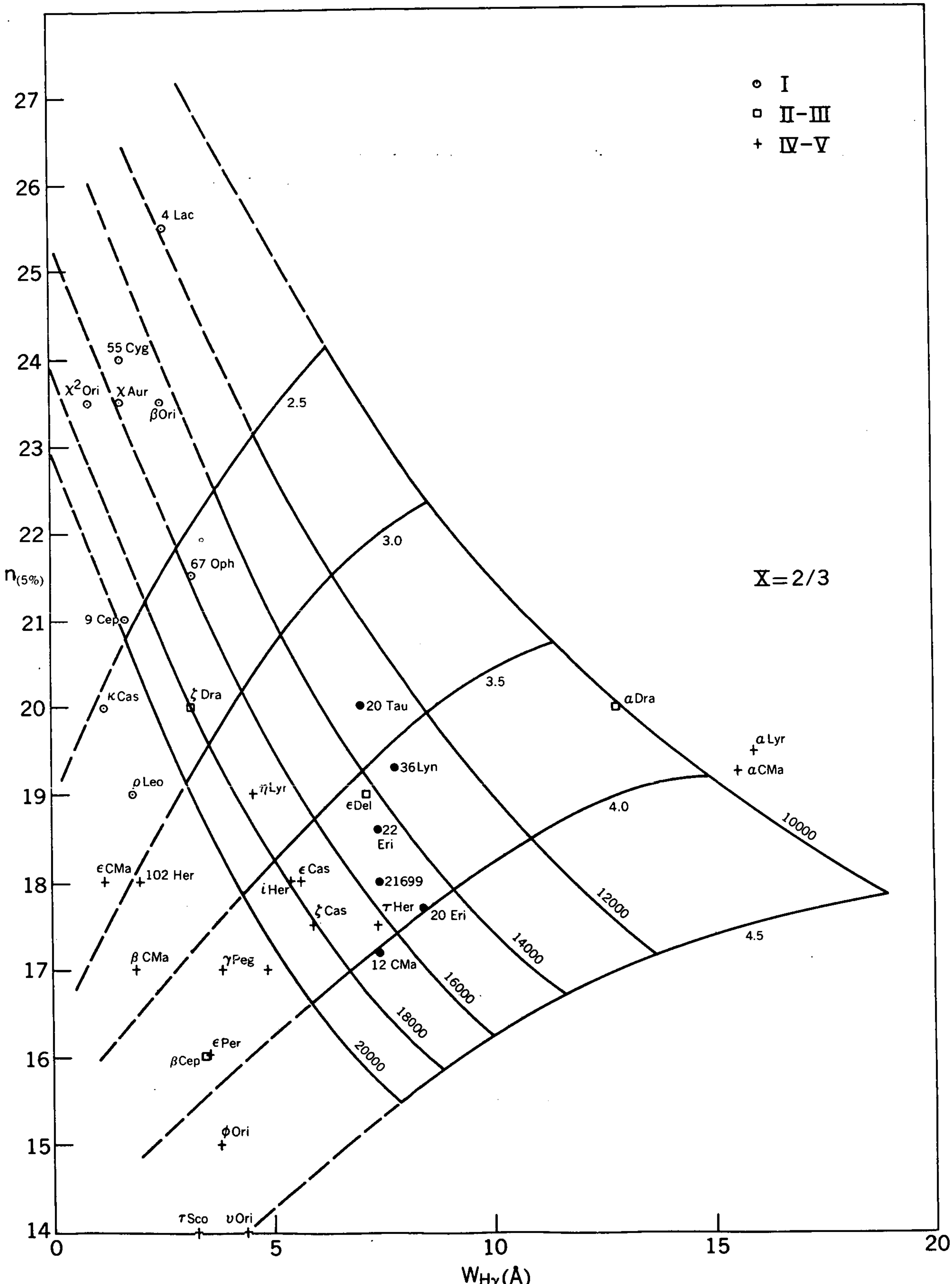

I
II–III
IV–V
X=2/3
27
26
25
24
23
22
21
20
19
18
17
16
15
14
$n_{(5\%)}$
0
5
10
15
20
$W_{H\gamma}$(Å)
2.5
3.0
3.5
4.0
4.5
10000
12000
14000
16000
18000
20000
4 Lac
55 Cyg
χ^2 Ori
χ Aur
β Ori
67 Oph
9 Cep
κ Cas
ζ Dra
ρ Leo
η Lyr
ϵ CMa
102 Her
i Her
ϵ Cas
ζ Cas
β CMa
γ Peg
β Cep
ϵ Per
ϕ Ori
τ Sco
υ Ori
20 Tau
36 Lyn
ϵ Del
22 Eri
21699
τ Her
20 Eri
12 CMa
α Dra
α Lyr
α CMa

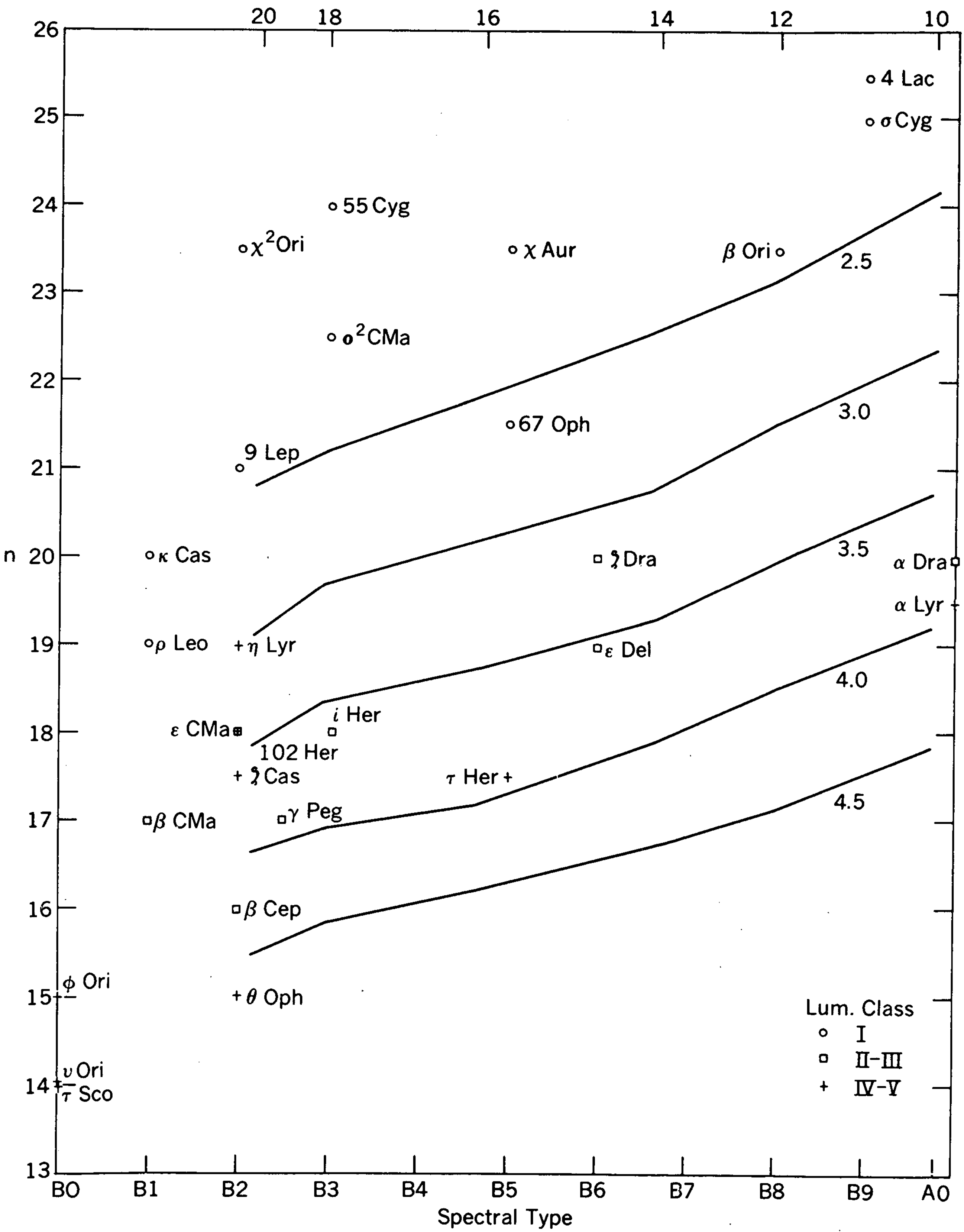

20
18
16
14
12
10
26
25
24
23
22
21
n 20
19
18
17
16
15
14
13
4 Lac
σ Cyg
55 Cyg
χ2 Ori
χ Aur
β Ori
2.5
o2 CMa
67 Oph
3.0
9 Lep
κ Cas
ζ Dra
3.5
α Dra
α Lyr
ρ Leo
η Lyr
ε Del
4.0
ε CMa
i Her
102 Her
ζ Cas
τ Her
4.5
β CMa
γ Peg
β Cep
φ Ori
θ Oph
Lum. Class
I
II-III
IV-V
υ Ori
τ Sco
B0
B1
B2
B3
B4
B5
B6
B7
B8
B9
A0
Spectral Type

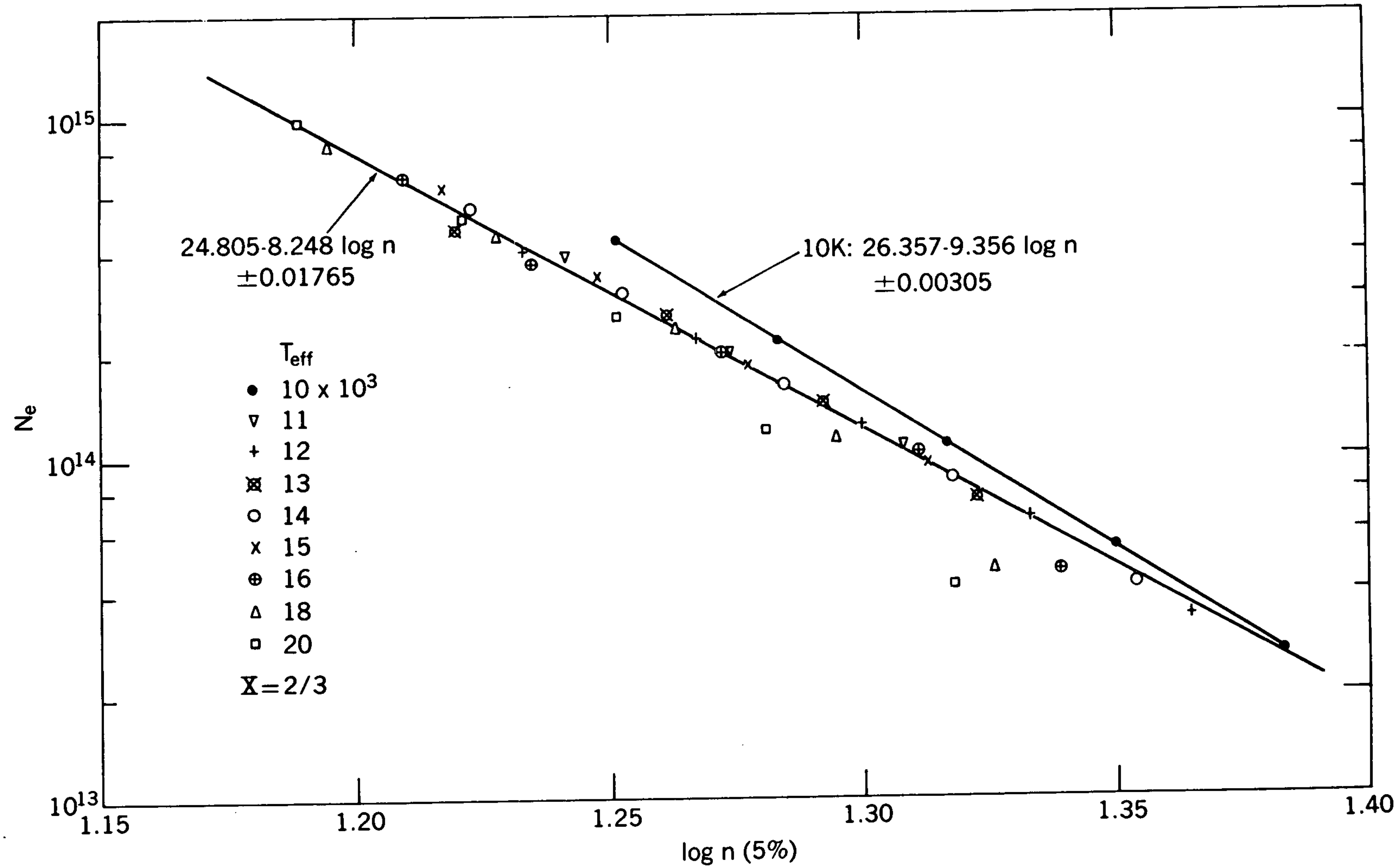
24.805-8.248 log n
±0.01765
10K: 26.357-9.356 log n
±0.00305
T_{eff}
10 x 10^3
11
12
13
14
15
16
18
20
X=2/3
N_e
10^{15}
10^{14}
10^{13}
1.15
1.20
1.25
1.30
1.35
1.40
log n (5%)